# Hydraulic Resistance of Soil Surface Seals in Irrigated Furrows

Antonius G. Segeren and Thomas J. Trout*

## ABSTRACT

**Soil surface seals resulting from overland flow in irrigation furrows reduce infiltration rates. A method was developed to quantify the hydraulic resistance of furrow seals. Infiltration was measured with a recirculating infiltrometer on two southern Idaho soils, Portneuf silt loam (coarse-silty, mixed, mesic Durixerollic Calciorthid) and Bahem loam (coarse-silty, mixed, mesic Xerollic Calciorthids). Surface sealing was prevented on half the furrow test sections with cheesecloth laid on the furrow perimeter. Subseal soil-water potential was measured with a recording tensiometer. A two-dimensional finite-difference infiltration model with measured flux as the wetted perimeter boundary condition calculated matric potential directly beneath the seal. Seal resistance was then calculated by Darcy's law from the measured flux and calculated potential. Surface sealing on the bare furrows decreased infiltration by an average of 46% compared with the cloth-covered furrows. The seal conductivity values, based on a constant seal thickness, decreased rapidly during the initial 100 min and reached 0.1 to 8% of the conductivity of the soil underlying the seal after 300 min. Potential gradients across the seal were inversely related to infiltration rate and the conductivity of the seal. The procedure successfully calculated seal conductivity changes with time and can be used to evaluate the effects of management practices on seal formation.**

INFILTRATION is a crucial factor affecting surface irrigation performance. This single parameter essentially controls not only the amount of water entering the soil, but also the advance rate of the overland flow. Overland flow applies shear forces to the soil surface. This causes soil aggregate breakdown and particle movement that can result in a thin low-conductivity depositional layer at the soil surface, commonly referred to as a soil surface seal.

Many researchers have studied the effects of rainfall and raindrop energy on surface sealing. Drop impact breaks down surface aggregates, compacts the surface layer, and washes fine particles into pores below the surface. These structural seals can greatly overshadow other factors affecting infiltration on unprotected soils (Moore, 1981). Glanville and Smith (1988) concluded that, in sealed soils, the surface seal rather than the water content of the soil profile determines the reduction in the infiltration rate. The extent of surface sealing is highly dependent on soil texture, with the silt content being a good indicator of the soil's susceptibility to surface sealing (Norton, 1987).

Stieb (1983) and Eisenhauer (1984) reported that soil surface seals also form as a result of overland flow. Eisenhauer (1984) showed that seals resulting from overland flow can reduce one-dimensional infiltration as much as 50%. Surface seals with overland flow result from surface soil aggregate breakdown caused by rapid wetting and the forces of the flowing water, and the deposition of sediment on the wetted perimeter. Larger sloughed or bed-load particles and microaggregates fill or cover larger pores. Smaller suspended seiment particles are filtered out at the surface as the water infiltrates and kept in place by the negative water-phase pressure below the soil surface (Brown et al., 1988). The tension that develops below a seal can also cause consolidation of the seal and the subseal layer, thus reducing the conductivity even further (Trout, 1990). Depositional seals are generally thin and lack a washed-in zone (Southard et al., 1988). Shainberg and Singer (1985) created depositional seals in the laboratory with hydraulic conductivities $<1\%$ that of the bulk soil when the electrical conductivity of the suspension was $<0.3$ dS/m.

The objectives of this study were to measure the effect of surface seal formation on furrow-irrigation infiltration under field conditions, and to develop a technique to quantify the hydraulic resistance of the developing seal. The technique would be useful to evaluate the effects of management practices on seal formation.

## METHODS

### Infiltration Simulation Model

A two-dimensional furrow infiltration model originally developed by Samani et al. (1985) was adapted to determine the hydraulic resistance of the soil surface seal as a function of irrigation (infiltration opportunity) time. The governing equation in the model is a two-dimensional form of the Richard's equation based on Darcy's law and the continuity equation for flow in porous media. The model uses the Brooks-Corey (1964) relationships to describe the functional relationships among matric potential, volumetric water content, and hydraulic conductivity for partially saturated soil. The Kirchoff transformation (Raats and Gardner, 1971) was applied to the governing equation to improve the numerical solution. The governing equation was solved by applying the Crank-Nicholson method (Crank and Nicholson, 1947). The Line Successive Over-Relaxation method (Remson et al., 1971) with an overrelaxation factor of 1.6 was used to solve the system of resulting equations instead of the SPARSE matrix method used by Samani et al. (1985). Segeren (1990) provides detailed information about the infiltration model.

The furrow cross section as assumed to be symmetric, so infiltration for only half of the cross section was simulated. The boundary conditions, shown in Fig. 1, were: (i) a no-flux boundary between the two symmetrical sides of the cross section, (ii) either a water depth (fixed potential) or a flux boundary along the wetted perimeter of the furrow, (iii) a no-flux boundary along the soil surface above the wetted perimeter, and (iv) an initial water-content boundary in the soil profile in front of the wetting front. Samani et al. (1985) and Segeren (1990) described the numerical approximations for the boundary conditions.

The most direct method to simulate the process of soil surface sealing is to model a two-layer soil profile in which the seal is the top layer. In this method, the hydraulic conductivity of the seal as a function of time is input to the computer model. The boundary condition along the wetted perimeter is the furrow water depth. To match measured infiltration data by this method, the changing conductivity

A.G. Segeren, Dep. of Agricultural and Irrigation Engineering, Utah State Univ.; and T.J. Trout, USDA-ARS Soil and Water Management Research, 3793 N 3600 E, Kimberly, ID 83341. Received 14 May 1990. *Corresponding author.

Published in Soil Sci. Soc. Am. J. 55:640–646 (1991).

of the seal during seal formation has to be determined by iteration at each time step. Also, the large change in potential gradient at the curved interface of the soil surface seal and the soil causes numerical problems. Because of these difficulties, an indirect approach was used.

In the direct approach, the seal is not treated as part of the soil profile but is simulated numerically as a boundary. With the measured flux through the wetted-perimeter seal set as a boundary condition, the model calculates the resulting matric potentials throughout the soil profile, including at the wetted-perimeter boundary, which is the interface between the seal and the subseal soil. The conductivity of the seal can then be calculated by Darcy's law:

$$K_s = -q\left(\frac{\Delta n}{\Delta p + \Delta z}\right) \approx -q\left(\frac{\Delta n}{\Delta p}\right) \qquad [1]$$

where:

$K_s$ = seal hydraulic conductivity (m/h)

$q$ = flux through the seal (m/h)

$\Delta z$ = change in gravitational potential across the seal (m)

$\Delta p$ = change in matric potential across the seal (m)

$\Delta n$ = seal thickness (m)

Since the matric-potential gradient across the typically thin seal will usually be much larger than the gravity gradient, the gravitational component can be dropped in Eq. [1]. Seal thickness, $\Delta n$, is highly variable, changes with time, and is difficult to measure. Thus the hydraulic resistance, $R$ (Swartzendruber, 1960), defined as:

$$R = \frac{\Delta n}{K_s} \approx -\frac{\Delta p}{q} \qquad [2]$$

is used to describe the resistance of the seal to flow regardless of thickness.

Two simplifying assumptions are required for this indirect procedure: (i) the surface seal is saturated from the start, and (ii) the hydraulic resistance of the seal is the only soil hydraulic parameter that changes after the start of the irrigation. The seal is not assumed to form instantly, but whatever seal is present is assumed to be saturated from the start. Moore (1981) found that the surface seal became saturated quickly after the beginning of the irrigation. Failure of this assumption will have little effect on the results. The second assumption requires all soil characteristics that affect infiltration (subseal saturated hydraulic conductivity, $K$, air-entry value, and pore-size distribution index) to be constant for the underlying soil.

The flux into the soil is assumed uniform along the wetted perimeter of the furrow and is calculated as the infiltrated volume per unit time divided by the furrow length and wetted perimeter. The use of an average flux along the wetted perimeter results in an average value computed for the resistance of the wetted-perimeter seal.

A sensitivity analysis (Segeren, 1990) showed that the model's calculation of matric potential at the wetted-perimeter boundary (and thus the calculated hydraulic resistance of the seal) is relatively insensitive to the initial soil water content and all the soil hydraulic parameters except the saturated hydraulic conductivity (moderately sensitive) and the air-entry value (highly sensitive) of the subseal soil. A 50% error in soil saturated conductivity results in a 20% error in the calculated $R$ value. The sensitivity to the air-entry value is a result of the nature of the Brooks-Corey relationship. This parameter can be determined within a relatively small confidence interval.

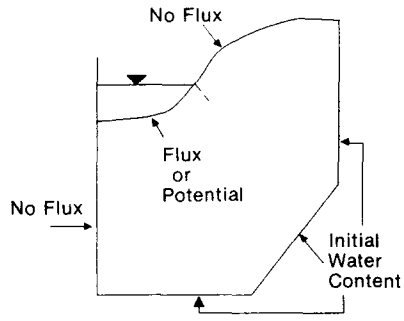


Fig. 1. Infiltration model boundary conditions.

## Field Data Collection

Furrow-infiltration measurements were made with a recirculating infiltrometer, which precisely measures infiltration in short furrow sections under near-normal field conditions. The recirculating infiltrometer used in this research was described by Blair and Trout (1989) and is shown in Fig. 2. The infiltrometer consisted of a small, long-throated V-furrow flume that served both as an inflow sump and for flow-rate measurement, a pump that lifted the flow from the downstream sump into the return reservoir, and a 500-L constant-head water-supply reservoir equipped with a Marriotte syphon, which maintained a constant water level in the return reservoir. From the return reservoir, the water flowed through a hose to the flume at the upper end of the furrow by gravity. A valve at the reservoir outlet regulated the flow rate in the furrow. The system maintained a constant flow rate and water volume in the recirculation system so that infiltration was equal to the water volume (depth) decrease in the supply reservoir with time. A pressure transducer (Model 152, Robinson-Halpern Co.[1], Plymouth Meeting, PA) connected to a multichannel data logger (Omnidata Easy Logger, Omnidata Int., Logan, UT) recorded the water depth in the supply reservoir every 5 min.

Brown et al. (1988) found that much of the sediment in furrows consisted of bedload aggregates and that fine sediment in the irrigation water enhanced soil surface seal formation. For that reason a low-speed (about 50 rpm) Archimedes screw was used to lift the sediment-laden water from the downstream sump to the return reservoir. This device lifted the water gently, thus minimizing the breakdown of sediment aggregates in the water. The system design prevented sediment deposition in this system so that all sediment flowing off the downstream end of the furrow was reintroduced with the water at the upstream end. After several passes of the water through the furrow section, sediment conveyed in the recirculating water was similar to that which would be conveyed in the mid or tail portions of a flowing furrow.

The flume and the downstream sump were installed to create near-normal furrow flow depth (and thus velocity) throughout the furrow section. Initial 6 L/min flow rates advanced the furrow stream at about 3m/min through the 6-m-long furrow section, allowing the soil to wet at a moderate rate. Once the water had reached the end of the furrow, the flow rate was increased to 20 L/min for the duration of the 6- to 8-h-long tests.

Soil-water potential was measured beneath the furrow with a tensiometer (Fig. 3) that consisted of a porous ceramic cup connected via a 1.5-mm nylon tube to a Microswitch 164 pressure transducer (Microswitch, Freeport, IL). Since the transducer is configured to measure positive pressure, it was

[1] Names of equipment manufacturers and suppliers are provided for the benefit of the reader and do not imply endorsement by the USDA or Utah State University.

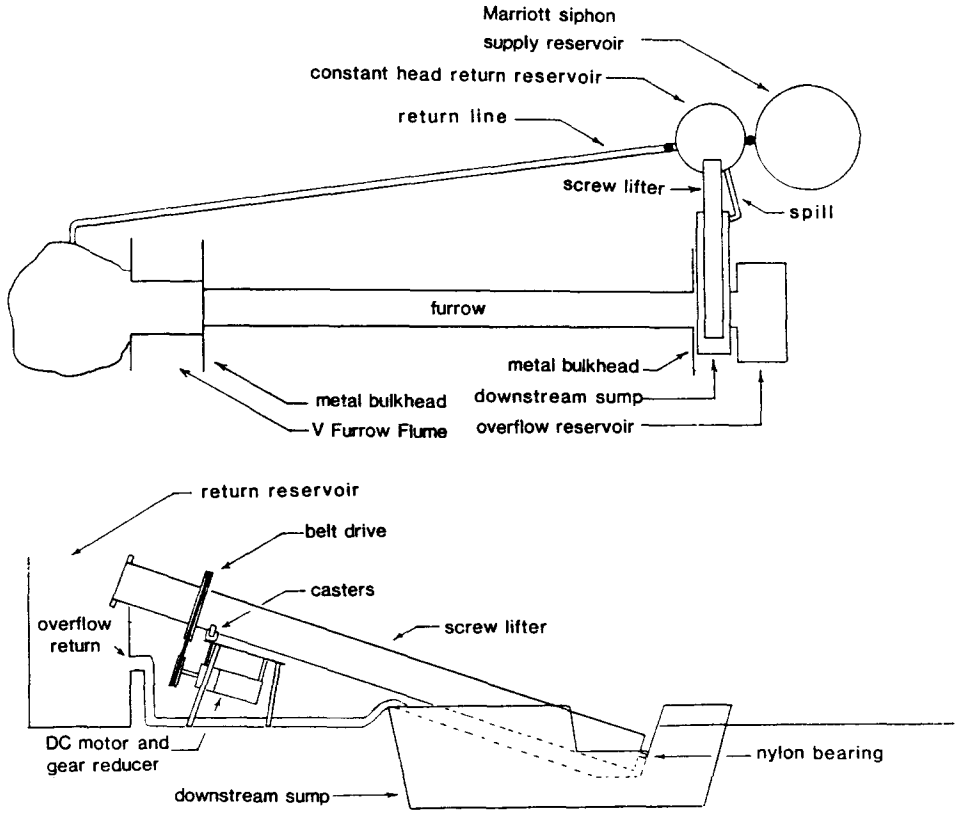


Fig. 2. Recirculating infiltrometer (after Blair and Trout, 1989).

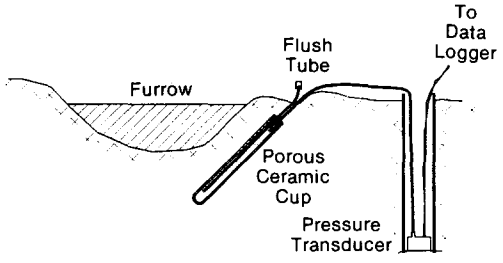


Fig. 3. Schematic of the tensiometer (from Trout, 1990).

placed below the soil surface in a small access tube. The reference pressure was measured with the ceramic cup laying in the flowing water adjacent to the measurement location at the beginning and end of each test. The difference between measured pressure in the soil and the reference pressure represents the total potential (gravity plus matric) referenced to the furrow-water surface. The 90-mm-long and 10-mm-diam. ceramic cup was inserted into the wetted soil at an angle such that it was about 20 mm from the furrow perimeter for most of its length.

Infiltration tests were run simultaneously in paired, non-wheel-furrow sections. One of the paired sections was left bare so that a normal surface seal would form. In the other section, a double layer of cheesecloth was laid on the perimeter of the furrow to absorb the shear forces of the flowing water and reduce sediment movement and seal formation. The cheesecloth was held in place by nails above the wetted perimeter and by a small steel rod laid along the center of the furrow bed. The hydraulic resistance of the cheesecloth was very low so it did not limit infiltration.

Thirty infiltration data sets were collected on two soils in southern Idaho. Table 1 lists relevant properties of the soils. The Portneuf silt loam site was at the USDA-ARS Kimberly, Idaho, Research Center. The Bahem loam soil was 5 km northeast of the research center. The slope of the furrows varied from 0.007 to 0.01 m/m. Except as noted, the furrows had not been irrigated since primary tillage (first irrigations). Irrigation water for both sites originated from the Snake River (electrical conductivity $\approx$ 0.05 S/m, Na adsorption ratio $<$ 1, sediment concentration $<$50 g/m$^3$).

The Brooks-Corey parameters (air-entry value, residual saturation, and pore-size distribution index) for both soils, determined from water-release data taken in the laboratory (Klute, 1986) are listed in Table 1. Initial soil profile water contents were gravimetrically measured before the irrigation. The saturated hydraulic conductivity of the soil profile was determined for each test section by trial-and-error selection of $K$ in the computer model (with a potential boundary at the wetted perimeter) until the model output closely matched measured cumulative infiltration data from the no-seal furrow. The procedure assumed a uniform and constant saturated conductivity throughout the profile and the results supported this assumption. Seal hydraulic-resistance values were then determined by the procedure described above, using measured infiltration into the seal furrows and model-generated subseal potentials [Eq. 2].

## RESULTS

### Field Experiments

The cheesecloth appeared to successfully inhibit furrow surface seal formation. The recirculating water in the cloth-covered furrows was clear, while the water in the bare furrows carried large concentrations of sediment. For the Portneuf soil, average sediment concentrations after approximately 30 min of irrigation

**Table 1. Soil properties and measured hydraulic parameters for the two test sites (0–0.3-m depth).**

| Property | Portneuf silt loam | Bahem loam |
|---|---|---|
| Sand (%) | 18 | 36 |
| Silt (%) | 61 | 48 |
| Clay (%) | 21 | 16 |
| Cation-exchange capacity ($cmol_c/kg$) | 18–23 | 18–23 |
| Exchangeable Na percentage (%) | <1 | <1 |
| Porosity ($m^3/m^3$) | 0.63 | 0.44 |
| Residual saturation ($m^3/m^3$) | 0.19 | 0.30 |
| Air-entry pressure (mm $H_2O$) | 120 | 150 |
| Pore-size distribution index | 0.55 | 0.30 |
| Initial water content ($m^3/m^3$) | | |
| Surface (0–20 mm) | <0.05 | <0.05 |
| Subsurface (50–300 mm) | 0.17–0.20 | 0.18–0.22 |

**Table 2. Mean and coefficient of variation (CV) of measured cumulative infiltration after 60 and 300 min of irrigation ($Z_{60}$ and $Z_{300}$) and infiltration rate after 300 min ($I_{300}$) for the four sets of infiltrometer tests.**

| | $Z_{60}$ | | $Z_{300}$ | | $I_{300}$ | |
|---|---|---|---|---|---|---|
| | Mean | CV | Mean | CV | Mean | CV |
| | L/m | | L/m | | L/(m h) | |
| Portneuf silt loam: | | | | | | |
| Field 1 ($n$ = 8) | | | | | | |
| seal | 22.4 | 0.31 | 51.6 | 0.30 | 6.0 | 0.23 |
| no seal | 29.5 | 0.26 | 84.0 | 0.28 | 12.2 | 0.28 |
| Field 2 ($n$ = 10) | | | | | | |
| seal | 19.1 | 0.13 | 42.4 | 0.16 | 4.7 | 0.28 |
| no seal | 29.2 | 0.13 | 88.1 | 0.13 | 12.8 | 0.14 |
| Field 2–2nd irrig. ($n$ = 8) | | | | | | |
| seal | 11.3 | 0.12 | 25.8 | 0.08 | 3.3 | 0.12 |
| no seal | 18.1 | 0.13 | 49.3 | 0.16 | 6.5 | 0.43 |
| Bahem loam: ($n$ = 4) | | | | | | |
| seal | 24.8 | 0.17 | 60.8 | 0.26 | 7.4 | 0.35 |
| no seal | 34.3 | 0.21 | 112.3 | 0.28 | 16.4 | 0.41 |

were 350 $g/m^3$ for the cloth-covered furrows and 2500 $g/m^3$ for the bare furrows. For the Bahem loam, these concentrations were 230 and 950 $g/m^3$, respectively. In all furrows, the sediment concentration in the water decreased with time after 30 min, indicating that the transported sediment continued to deposit at the furrow perimeter. Cloth-covered furrow perimeters showed little shape change during the irrigation, while the cross sections of the furrows without the cheesecloth became wider and flatter. Although a smooth, slick seal was visually obvious on the bare furrow following irrigation, the cloth-covered furrow surfaces were rough and no seal was visible.

In all 30 paired tests, the bare furrow on which the normal seal was allowed to form (seal furrow) had lower cumulative infiltration after 60 min ($Z_{60}$) and 300 min ($Z_{300}$) of irrigation than the cheesecloth-covered (no-seal) furrow (Table 2). The average reduction in cumulative infiltration after 300 min was 46%. The infiltration rates after 300 min ($I_{300}$) were also lower for all the seal furrows with an average reduction of 57%. Note that infiltration was lower during the second irrigation, but the relative differences between seal and no-seal furrows were similar to the other tests. These no-seal furrows had also been cloth-covered during the first irrigations.

The cheesecloth created drag resistance to furrow flow, which increased the flow depth and wetted perimeter by about 20%. Thus, a small portion (less than one-quarter) of the 85 to 90% higher infiltration from the no-seal furrows could be attributable to the increase in wetted perimeter and potential at the soil surface.

**Table 3. Measured cumulative and final infiltration rates after 300 min of irrigation ($Z_{300}$ and $I_{300}$, respectively) for both seal and no-seal furrows, soil saturated hydraulic conductivity ($K$), and calculated final seal conductivity ($K_s$) and resistance ($R$) for seven selected data sets.**

| Soil test | No-seal furrow | | | Seal furrow | | | |
|---|---|---|---|---|---|---|---|
| | $Z_{300}$ | $I_{300}$ | $K$ | $Z_{300}$ | $I_{300}$ | Final $R$ | Final $K_s$ |
| | L/m | L/(m h) | mm/h | L/m | L/(m h) | h | mm/h |
| Portneuf | | | | | | | |
| 1 | 86 | 13.0 | 48 | 73 | 8.0 | 0.09 | 3.8 |
| 2 | 85 | 12.8 | 48 | 48 | 5.6 | 0.25 | 1.4 |
| 3 | 88 | 13.6 | 48 | 29 | 3.2 | 0.44 | 0.8 |
| 4 | 68 | 10.2 | 38 | 48 | 4.6 | 0.23 | 1.5 |
| 5 | 101 | 15.4 | 85 | 36 | 3.2 | 0.44 | 0.8 |
| Bahem | | | | | | | |
| 6 | 115 | 17.8 | 125 | 41 | 4.5 | 0.50 | 0.2 |
| 7 | 117 | 16.9 | 125 | 76 | 8.0 | 0.17 | 0.6 |

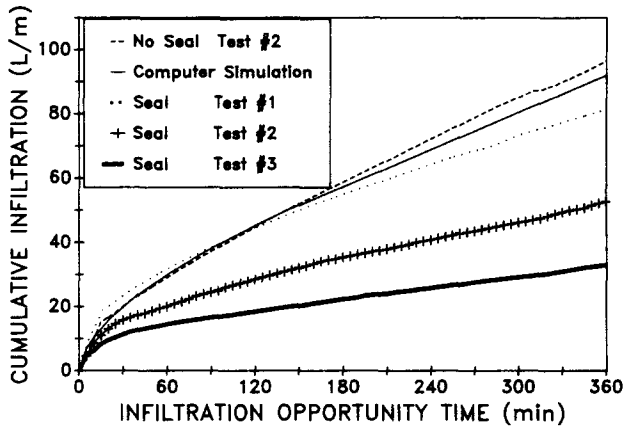


Fig. 4. Cumulative infiltration for tests no. 1 through 3 and simulated by the model with subseal saturated hydraulic conductivity = 48 mm/h.

Table 2 lists the coefficients of variation for the infiltration parameters for each set of tests. The CVs generally varied between 0.12 and 0.35. The relative infiltration variability of the seal furrows was not different from that of the no-seal furrows.

Infiltration parameters for seven individual pairs of tests are given in Table 3. These data sets were chosen to represent the average and range of measured infiltration. The first three pairs are first-irrigation tests on the Portneuf soil, which had near-average infiltration in the no-seal furrows and high, moderate, and low infiltration in the paired seal furrows. The cumulative infiltration curves for these tests are shown in Fig. 4. The fourth and fifth tests in Table 3 represent the same soil conditions with low and high measured infiltration in the no-seal furrows. The last two sets are for furrows in the Bahem loam soil with average no-seal infiltration and high and low seal-furrow infiltration. These seven data sets were used in the simulation tests.

Measured soil-water potential below the seal fur-

rows was consistently much lower than that below the cloth-covered furrows (Fig. 5). The potential gradient across the top 20 mm of soil with the seal was typically about four times larger than the gradient in the no-seal furrows after 300 min of irrigation. After the soil initially wetted, the potential beneath the seal generally decreased throughout the irrigation, with the most rapid decrease occurring during the first 2 h.

## Computer Simulations

Table 3 lists the constant soil saturated-hydraulic-conductivity values, $K$, with which the no-seal simulation model best matched the field-measured cumulative infiltration. Figure 4 shows the simulated infiltration with $K = 48$ mm/h. The average deviation between the field data and computer-simulated cumulative infiltration for all the no-seal tests was 7%. With the proper $K$ value, the computer model adequately matches measured no-seal infiltration. If the $K$ derived for the no-seal furrow is valid for the paired seal furrow, the model should simulate subseal water movement and potentials equally well for the seal case.

Figure 6 shows the matric potential distribution beneath the seal furrow generated by the model for the second test (Table 3) after 360 min of irrigation. The matric potential along the wetted perimeter just below the seal varied from −151 mm at the center of the furrow to −158 at the edge (water surface). When the effect of the 20-mm water depth in the furrow is considered, the potential drop across the seal varied from −171 mm at the center to −158 mm at the edge—only an 8% gradient variation. The large potential gradient through the thin seal justifies ignoring the gravity gradient [Eq. 1].

Figure 6 shows the matric potential in the area around the tensiometer varying between about −165 mm near the lower end to −190 mm near the upper end. Due to the length and angle of the tensiometer cup, the gravity potential (referenced to the water surface) would be about −60 mm at the lower end and 0 at the upper end of the tensiometer, resulting in a total potential varying between −225 to −190 mm. Thus, late in the irrigation, the total potential measured by the tensiometer is expected to be about 30 mm lower than the actual potential just below the seal. In Fig. 5, the total potential just below the seal (furrow center) computed by the model is shown along with the field tensiometer data for the second test. The match for this data set is closer than expected. Other comparisons presented by Segeren (1990) also show no consistent differences between the tensiometer-measured potential and the model-predicted potential just below the seal.

Figure 7 shows model-calculated matric-potential variation with time just below the seal for the first

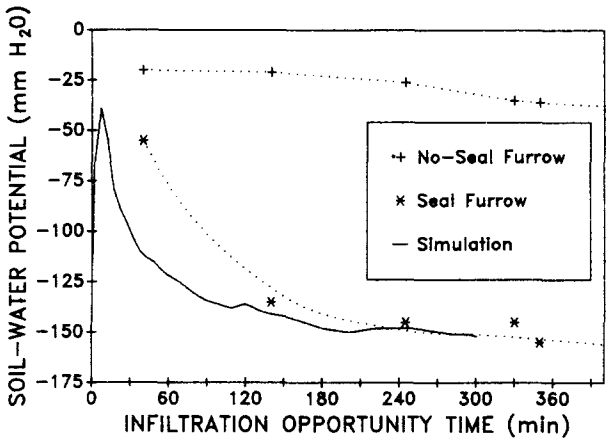


Fig. 5. Total potential measured beneath the furrow wetted perimeter and simulated just below the seal for test no. 2.

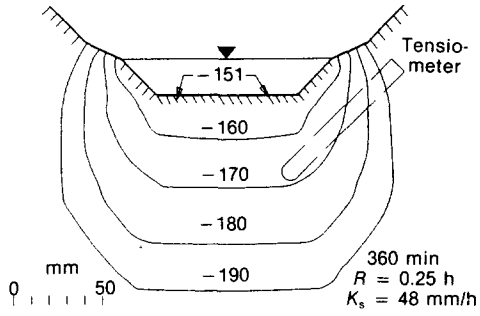


Fig. 6. Simulated matric potentials (mm $H_2O$) after 360 min of irrigation for test no. 2. $R$ is hydraulic resistance and $K_s$ is seal hydraulic conductivity.

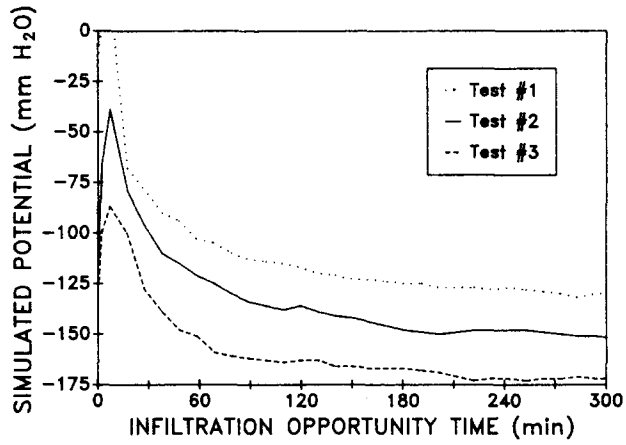


Fig. 7. Simulated soil-water potentials for tests no. 1 through 3.

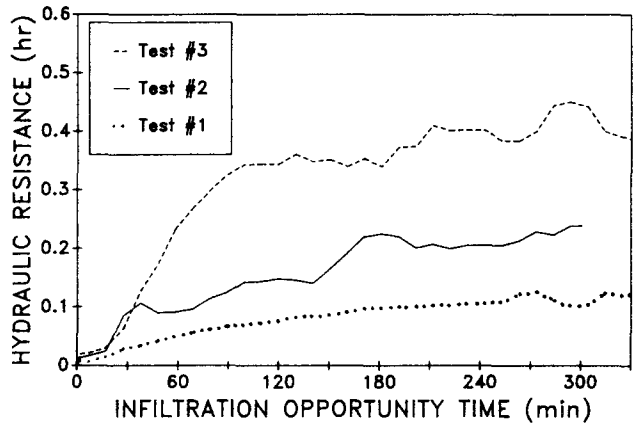


Fig. 8. Derived seal hydraulic resistance for tests no. 1 through 3.

through third tests (Table 3). The potentials show an initial rapid increase as the soil wets, then a rapid decrease during the first hour of infiltration as the seal forms and a continuing gradual decrease during the remainder of the irrigation. This continuing potential decrease shows that the seal resistance continues to increase throughout the irrigation. The figure shows, as expected, that the lower the flux, the lower the predicted potential at the interface between seal and soil and, thus, the higher the gradient through the seal.

Figure 8 shows the calculated seal hydraulic resistance as a function of time for the same three data sets. The resistance of the seal, in relative terms, increases rapidly during the first hour of irrigation. Although the resistance of the seal continually increases during each run, the gradually increasing hydraulic gradient shown in Fig. 7 results in the measured infiltration rate remaining relatively constant after the initial 150 to 200 min of irrigation. The short-term erratic fluctuations shown in Fig. 8 are the result of procedure-related fluctuations in the measured infiltration rate. As expected, the furrow with lowest infiltration resulted from the seal with the highest resistance.

Seal thickness for the two soils was estimated visually with the aid of a microscope on cores collected after irrigations. Seal thicknesses varied widely between 0.1 and 2 mm and averaged 0.35 and 0.12 mm for the Portneuf and Bahem soils, respectively. The average final seal hydraulic-conductivity values listed in Table 3 were calculated using these seal thicknesses ($K_s = \Delta n\ q/\Delta p$, Eq. 2). Final conductivity of the seal for the Portneuf soil ranged from 1 to 8% of that of the subsoil. For the average conditions (data set no. 2, Table 3), final seal conductivity was 3% that of the subseal soil. For the Bahem soil, the final seal conductivity was <1% that of the subseal soil. The lower calculated conductivity of the Bahem seal is primarily a result of the thinner measured seal thickness rather than lower seal resistance. Because of the wide variability in and imprecise measurement of seal thickness, little confidence can be placed in this difference.

Although infiltration is directly related to the conductivity of the seal, the relationship is not proportional, as might be assumed from a cursory analysis. A relative decrease in infiltration requires a larger relative increase in the seal hydraulic resistance. The data presented in Table 3 indicates that a 97% reduction in seal conductivity reduced the cumulative infiltration after 300 min by only 44% (from 85–48 L/m). The low conductivity of the thin seal is partially offset by the large hydraulic gradient that develops across the seal.

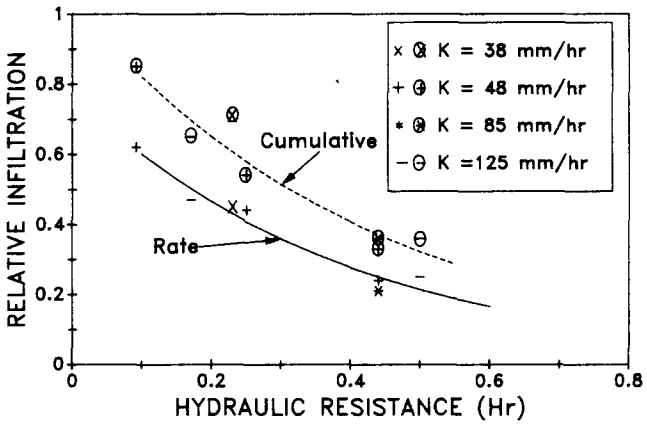


Fig. 9. Seal furrow cumulative infiltration and infiltration rate at 300 min, relative to infiltration with no seal, vs. seal hydraulic resistance. $K$ is subseal saturated hydraulic conductivity.

The influence of seal resistance on furrow infiltration is shown in Fig. 9, which shows infiltration, relative to infiltration with no seal, vs. the seal resistance. The lines in the figure follow exponential decay functions. The relative infiltration would be 1.0 when the resistance is equal to zero (no effect of the seal on infiltration) and will asymptotically approach zero as the resistance becomes large. The figure demonstrates the relatively larger resistance decrease required to decrease infiltration. For example, doubling the resistance from 0.1 to 0.2 results in only a 25% decrease in the infiltration rate. This results from the increase in potential gradient across the seal as the resistance increases.

The data points depicted in Fig. 9 appear to follow the same curves, even though the soil conductivities varied from 38 to 125 mm/h. This indicates that the seal has the same relative effect on infiltration regardless of the hydraulic conductivity of the subseal soil. Note, however, that this tendency would be accentuated by error in the assumption that the paired furrows have the same soil conductivity.

## DISCUSSION

In this procedure, the only soil physical change that affects infiltration is assumed to occur at the soil surface in the form of a thin surface seal. For the no-seal furrows, cumulative infiltration was successfully simulated with a constant saturated-hydraulic-conductivity value. Thus, structural changes for these soils as they wet under minimal sediment-movement conditions, such as aggregate sloughing and soil consolidation, apparently have little effect on infiltration or occur very rapidly so that their effects are difficult to isolate. The methodology used, however, does not eliminate the possibility that, with sediment movement and surface seal formation, physical changes occur below the thin surface layer. Processes such as consolidation and washing-in of sediment may reduce conductivity below the seal. The effects of any such processes are reflected in the computed seal-resistance value. Soil cores taken from furrow beds after two tests showed no visible porosity changes below the low-porosity surface seal layer.

The model simulations predict a relatively small matric-potential gradient beneath a furrow surface seal (Fig. 6). The same low gradient over a considerable depth beneath a low-conductivity layer was found by several other researchers for one-dimensional infiltration (Takagi, 1960, Hillel and Gardner, 1969). The model also predicted a fairly uniform potential beneath the seal along the wetted perimeter. These small subseal gradients indicate that a small tensiometer in-

stalled beneath the furrow seal is adequate to estimate potential in that region and, thus, the potential gradient across the seal. The good agreement between potentials measured in the field and simulated by the model support this thesis. Thus, except early in the irrigation when moisture and therefore potential gradients near the seal are large, the simulation model is not required to estimated soil-water potential beneath the seal. Seal resistance can be approximated fairly well by applying Darcy's law to subseal tensiometer-measured potentials and infiltration flux. This procedure will enable more efficient comparative evaluation of the effect of management practices on surface seal formation.

Hydraulic conductivity is a more commonly used and theoretically useful term than hydraulic resistance. However, the surface seal thickness values required to calculate the seal saturated hydraulic conductivity were difficult to measure and highly variable. The seal thickness is expected to increase with time, especially during the first 2 h of the irrigation, but soil cores to evaluate seal thickness are difficult to collect until after the irrigation has ended. The effective seal could also be composed of several layers with varying conductivity. Since the net effect of the seal on infiltration is a function of the ratio of the seal conductivity and the seal thickness, determining the variation in either component will provide essentially the same information. Consequently, hydraulic resistance (or its reciprocal, hydraulic conductance) is a more practical and useful parameter than hydraulic conductivity to characterize the effects of the seal on infiltration.

## REFERENCES

Blair, A.W., and T.J. Trout. 1989. Recirculating furrow infiltrometer design guide. Tech. Rep. CRWR 223. Center for Research in Water Resources, Univ. of Texas, Austin.

Brooks, R.H., and A.T. Corey. 1964. Hydraulic properties of porous media. Hydrol. Pap. no. 3. Colorado State Univ., Fort Collins.

Brown, M.J., W.D. Kemper, T.J. Trout, and A.S. Humpherys. 1988. Sediment, erosion and water intake in furrows. Irrig. Sci. 9:45–55.

Crank, J., and P. Nicholson. 1947. A practical method for numerical integration of solutions of partial differential equations of the heat conduction type. Proc. Cambridge Philos. Soc. 43:50–67.

Eisenhauer, D.E. 1984. Surface sealing and infiltration with surface irrigation. Ph.D diss. Colorado State Univ., Fort Collins (Diss. Abstr. 84–17087).

Glanville, S.F., and G.B. Smith. 1988. Aggregate breakdown in clay soils under simulated rain and effects on infiltration. Aus. J. Soil Res. 9:668–675.

Hillel, D., and W.R. Gardner. 1969. Steady-state infiltration into crust-topped profiles. Soil Sci. 109:69–76.

Klute, A. 1986. Water retention: Laboratory methods. p. 635–662. *In* A. Klute (ed.) Methods of soil analysis. Part 1. 2nd ed. Agron. Monogr. 9. ASA and SSSA, Madison, WI.

Moore, I.D. 1981. Effects of surface sealing on infiltration. Trans. ASAE 24:1546–1552.

Norton, L.D. 1987. Micromorphological study of surface seals developed under simulated rainfall. Geoderma 40:127–140.

Raats, P.A.C., and W.R. Gardner. 1971. Comparison of empirical relationships between pressure head and hydraulic conductivity and some observations on radially symmetric flow. Water Resour. Res. 7:921–928.

Remson, I., G.M. Hornberger, and F.J. Molz. 1971. Numerical-methods in subsurface hydrology. Wiley-Interscience, New York.

Samani, Z.A., W.R. Walker, R.W. Jeppson, and L.S. Willardson. 1985. Numerical solution for unsteady two-dimensional infiltration in irrigation furrows. Trans. ASAE 28:11876–1190.

Segeren, A.G. 1990. The hydraulic conductivity of a soil surface skin formed by furrow flow. Ph.D diss. Utah State Univ., Logan (Diss. Abstr. 90-34091).

Shainberg, I., and M.J. Singer. 1985. Effect of electrolytic concentration on the hydraulic properties of depositional crusts. Soil Sci. Soc. Am. J. 49:1260.

Southard, R.J., I. Shainberg, and M.J. Singer. 1988. Influence of electrolyte concentration on the micromorphology of artificial depositional crust. Soil Sci. 145:278–288.

Stieb, J.S. 1983. Surface seal development with shallow overland flow. M.S. thesis. Colorado State Univ., Fort Collins.

Swartzendruber, D. 1960. Water flow through a soil profile as affected by the least permeable layer. Geophys. Res. 65:4037–4042.

Takagi, S. 1960. Analysis of the vertical downward flow of water through a two-layered soil. Soil Sci. 90:98–103.

Trout, T.J. 1990. Surface seal influence on surge flow furrow infiltration. Trans. ASAE 33:1538–1589.